Chapter 2
Charged Particle-Beam Acceleration and Lasers: Contextualizing Technologies that Shaped Electronic Warfare

2.1 Introduction

In 1931, Nikola Tesla, famous inventor and the father of alternating current (AC), publicized at a media conference that he was on the brink of discovering and presenting a totally new source of energy. Regarding this invention, he stated: "*The idea first came upon me as a tremendous shock … I can only say at this time that it will come from an entirely new and unsuspected source*". Nikola Tesla was known to be strongly anti-war and his inventions were inspired by the desire to put an end to warfare. By 1937 war in Europe was inevitable, as tensions were rising, and World War II started in September 1939. A discouraged Tesla distributed his technical paper titled, "*New Art of Projecting Concentrated Non-Dispersive Energy through Natural Media*" to the United States, Canada, England, France, the Soviet Union and Yugoslavia to generate interest and financing for his idea. This paper described a method (although never implemented) to direct high-velocity air through an open-ended vacuum chamber; today the basis of charged particle beam weapons. The first research conducted to realize a DEW, a particle beam accelerator aimed at incoming missiles, was undertaken in 1958 by the Advanced Research Projects Agency (ARPA, founded in 1958), two years before the successful demonstration of the laser built by Theodore H. Maiman at Hughes Research Laboratories (the research arm of Hughes Aircraft, established in 1960). A charged particle-beam accelerator, as the name suggests, uses EM fields to accelerate ionized particles to nearly the speed of light and to contain these particles in a narrow, defined beam. A laser emits coherent radiation in a narrow and diffraction-limited beam.

This chapter describes the principles of operation of charged particle-beam acceleration and its potential applications in EW, followed by the principles of operation of lasers and its uses in EW and other military applications.

© Springer International Publishing AG 2017

W. Lambrechts and S. Sinha, *SiGe-based Re-engineering of Electronic Warfare Subsystems*, Signals and Communication Technology,
DOI 10.1007/978-3-319-47403-8_2

2.2 Charged Particle-Beam Accelerator

The history of charged particle-beam accelerators (shortened to particle accelerators in this book) arguably began with the evacuated tube and spark coil of W.K. Roentgen, which accelerated electrons and resulted in the discovery of X rays in 1895 (Woodyard 1948). In 1897, J.J. Thomson discovered the electron using a particle accelerator known as a cathode ray tube by measuring the mass of the cathode rays and showing that the rays consisted of negatively charged particles smaller than atoms. Ernest Rutherford discovered in 1911 that an atom has a positive center, which contains most of its mass, and in 1920 proposed that the particles be called protons. A few years later, in 1932, James Chadwick was able to prove that the nucleus of an atom also contained a neutral particle, later called the neutron. Charged particle-beam accelerators are designed to accelerate protons to speeds approaching the speed of light; primarily to collide the particles against one another and study the collision (particle physics). Particle accelerators can be classified into three categories by adapting the work of Woodyard (1948), namely firstly according to the form factor of the accelerator, secondly according to the electric principles used to obtain an electric field in the generator, and thirdly according to the types of particles that are accelerated. These categories are depicted in Fig. 2.1.

As seen in Fig. 2.1, each category can be subdivided into two types. The form factors of the typical generators include linear and circular devices. To obtain a strong electric field, either direct current (DC) static fields or AC electric fields can be used. Distinguishing between the two types of particles that can be accelerated involves using light or heavy particles.

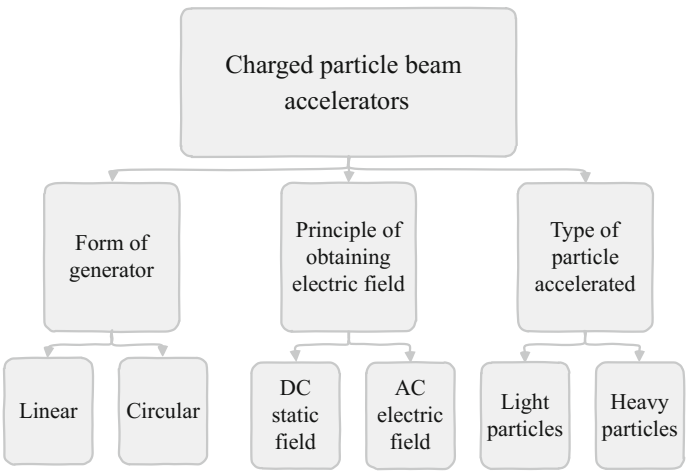

Fig. 2.1 Classifying the categories of charged beam particle accelerators (adapted from Woodyard 1948)

Linear accelerators push charged particles along a straight line through an electric field. The energy transferred to the particle is related to the length of the device and the voltage slope along its path. The Van De Graaff generator is an example of a linear particle accelerator.

Circular accelerators work on a similar principle, except that the particles travel around a circular path, allowing for smaller devices' routing particles to complete many revolutions within the same path. Electromagnets guide the particles in circular paths. Circular accelerators include the cyclotron, betatron and synchrotron. Cyclotrons, first conceived in Germany in the late 1920s, are the earliest operational circular accelerators. The first operating cyclotron was invented by E. O. Lawrence in 1929 at the University of California, Berkeley. Cyclotrons were the most powerful particle accelerators until the 1950s, superseded by the betatron and synchrotron. Particles are kept on a spiral trajectory by a DC static magnetic field and accelerated by a high-frequency RF electric field. The RF field is applied to two D-shaped sheet metal electrodes inside a vacuum chamber. These electrodes are placed face to face with each other with a narrow gap between them. Charged particles are injected into the center of this space. Electromagnets perpendicular to the electrode plane cause the particles to bend in a circle because of the Lorentz force perpendicular to their direction of motion. Synchrotrons synchronize to a particle beam of increasing kinetic energy to bend the charged particles into a closed path. A synchrotron therefore varies the strength of the magnetic field in time according with the particle gain energy, as opposed to varying the field in space. Synchrotrons typically receive pre-accelerated proton particles from cyclotrons or lower-energy synchrotrons. Betatrons, invented in 1940, accelerate the charged particles by induction from an increasing (similar to synchrotrons) magnetic field. The particles behave as if they are the second winding of a transformer and accelerate owing to the change in magnetic flux through its circular orbit.

A guideline of the required kinetic energy (K) in eV to accelerate a proton with rest mass of 0.938 GeV/c^2, where c is the speed of light (299,792,458 m/s), to a percentage of the speed of light is given by the European Organization for Nuclear Research (CERN), in a summary of the accelerators used at CERN (2009). These values are given in Table 2.1.

In Table 2.1, the linear accelerator 2 (Linac 2) at CERN generates 50 meV kinetic energy to accelerate proton particles to 31.4 % of the speed of light. The proton synchrotron booster (PS booster) is able to accelerate particles to 91.6 % of

Table 2.1 Relationship between the required kinetic energy and speed of a proton, achieved by CERN machines only (adapted from CERN 2009)

Kinetic energy of a proton (K)	Speed (percentage of speed of light)	Accelerator
50 meV	31.4	Linac 2
1.4 GeV	91.6	PS Booster
25 GeV	99.93	PS
450 GeV	99.9998	SPS
7 TeV	99.9999991	LHC

the speed of light using 1.4 GeV energy. The proton synchrotron (PS) accelerates proton particles either received from the PS booster or heavy ions from the low energy ion ring (LEIR) to reach 99.93 % of the speed of light by applying 25 GeV of kinetic energy. The super PS provides particle beams for the large hadron collider (LHC) at 450 GeV to achieve 99.9998 % of the speed of light, amplified to a total of 7 TeV in the LHC to reach 99.9999991 % of the speed of light. It is theoretically not possible to accelerate a particle with mass (m) to the speed of light. This can be mathematically presented by using Einstein's theory of relativity, where a particle's energy (E) is described by

$$E = \frac{mc^2}{\sqrt{1 - v^2/c^2}} \tag{2.1}$$

where v is the velocity of the particle along the axis of its movement (along a vector $\boldsymbol{r}$). If the velocity of the particle is zero, (2.1) simplifies to Einstein's equation of the theory of relativity for a particle at rest, given as

$$E = mc^2. \tag{2.2}$$

No particle with a non-zero mass can reach the speed of light, no matter how much energy is added to the particle. Famously, Einstein (1905) proposed that "*If a body gives off the energy L in the form of radiation, its mass diminishes by* L/c^2". Einstein used the letter L for energy and in subsequent work the symbol E was used to rewrite it in the form $E = mc^2$. In (2.2), c is constant, therefore adding energy to the particle increases its mass. By theoretically increasing the energy infinitely the mass of the particle would proportionally also increase infinitely, which is practically impossible and it cannot reach the speed of light by applying this principle. If the particle is moving, it has kinetic energy (K) and the total energy of the particle is the sum of its rest energy and its kinetic energy, given by

$$E = mc^2 + K. \tag{2.3}$$

The kinetic energy of the particle can be calculated by rearranging (2.3) to

$$\begin{aligned} K &= E - mc^2 \\ &= mc^2 \left(\frac{1}{\sqrt{1 - v^2/c^2}} - 1 \right). \end{aligned} \tag{2.4}$$

If the velocity of the particle is much lower than the speed of light ($v \ll c$), then the kinetic energy in (2.4) can be simplified to

$$K \approx \frac{1}{2} mv^2 \tag{2.5}$$

which will be transferred to any object that it collides with at this speed, called the translational kinetic energy (E_t). Nature produces the highest energies compared to any anthropogenic particle accelerators in the form of cosmic rays. The most energetic cosmic ray ever observed was a proton accelerated in excess of 1×10^{20} eV and the source of such ultrahigh energy cosmic rays is still being investigated. In nuclear and particle physics, particle accelerators have contributed in many inventions, discoveries and applications.

The LHC beneath the border between France and Switzerland built by CERN is a 17 mile (27 km) long circular tunnel with depths ranging from 164 to 574 ft (50–175 m) underground. It uses superconducting magnets and is the largest particle collider in the world. The LHC can potentially generate a total of 14 TeV (two high-energy particle beams generating 7 TeV of energy in ultrahigh vacuum each) of energy to accelerate and collide protons. Initial tests of the LHC were conducted at lower energy levels following a magnet quench incident, which damaged the superconducting magnets. The proton collisions are studied at four research stations of the LHC, named CMS, ATLAS and LHCb to investigate the particles that are detected during the collisions. One of the largest drives for building the LHC was the aspiration to find and identify the Higgs boson, which would prove or disprove theories such as supersymmetry and the existence of the multiverse. A Higgs boson of mass 125.3 GeV was identified on 4 July 2012 through experiments (initially estimated at 115 GeV to support the theory of supersymmetry or at 140 GeV to support the theory of a multiverse) on the LHC; however, scientists are still confirming whether this discovery is the true Higgs boson or if there is a possibility that multiple Higgs bosons may exist.

In Barbalat (1994) several examples of applications of particle accelerators are described. These applications are still in use today, with additional uses especially in scientific research emerging. These applications are listed in Table 2.2.

The applications and benefits of particle accelerators, as shown in Table 2.2, have been expanding with advances in technology in recent years. The operating principle of particle acceleration remains constant. Current research focused on electron and proton/ion particle acceleration through lasers to unprecedented energies in the high GeV range is receiving high amounts of attention. Research activity in this field aims to accomplish the development of high-quality and low-cost, versatile and small form-factor proton sources for research, medical applications and EW. In an article published by Extreme Light Infrastructure, the following abstract is taken from the website: *"... the dramatic rise in attainable laser intensity has generated an even more dramatic emergence and now evolution of the fields of research associated with non-linear laser-matter interaction. Production and acceleration of electrons up to 1 GeV over accelerating distances around 1 mm (100 meters for conventional accelerators) and hadron acceleration to 100 meV, are the clearly visible results of this evolution*". The increases in brightness and decrease in pulse duration of particle beams are methods to significantly change and improve on the investigation of particle matter, which will also lead to improvements and new applications of particle acceleration. Berkeley Labs published a world record in December 2014 for a compact particle accelerator

Table 2.2 Applications of particle accelerators (adapted from Barbalat 1994)

Field	Examples of applications
Scientific research	Nuclear physics (exploring the nucleus) Particle physics (building blocks of matter) Cosmology and astrophysics (cosmic observations) Atomic physics Condensed matter physics Chemistry/biology (chemical characteristics of molecules/cancer therapy)
Industrial applications	Semiconductor ion implanting Micro-photolithography Material surface modification Plasma-etching Scanning electron microscopes
Medicine	X-rays Nuclear magnetic resonance (used in X-rays) Gamma-ray therapy Neutron/heavy charged particle therapy Positron emission tomography Deoxyribonucleic acid (DNA) research
Radiation	Food preservation Sterilization of toxic waste Polymerization of plastics Explosive detection
Power engineering	Nuclear waste disposal Inertial confinement fusion Plasma heating

using a powerful laser (Berkeley Lab Laser Accelerator—BELLA) to accelerate subatomic particles to 4.25 GeV in a 3.54 inch (9 cm) long tube. The traditional means of accelerating particles by use of electric fields have a limit of approximately 100 meV per meter, as is the case for the LHC at CERN. Laser acceleration of subatomic particles have clearly overcome this limitation by an order of magnitude. Laser accelerators (also referred to as laser-plasma accelerators) inject a laser light into a short and thin cavity, which contains a specific plasma. The beam effectively creates a channel through the plasma as well as waves that trap free electrons and accelerate them to high energies. The acceleration gradient, $E_{A,}$ for a linear plasma wave can be determined by

$$E_A = c\sqrt{\frac{m_e \rho}{\varepsilon_0}} \tag{2.6}$$

where c is the speed of light in a vacuum, m_e is the mass of an electron, ρ is the plasma density in particles per cubic meter and ε_0 is the permittivity of free space.

As an introduction to DEW and particle-beam weapons, the concept of lasers is discussed in the following sections. A primary goal of this book is to explore and research the advantages and possibilities of using SiGe in various aspects of EW.

Its significance becomes apparent when considering the principles behind the technologies that enable it to make a contribution in these areas. Radar principles are also crucial to understand, interpret, highlight and identify the possibilities of SiGe as enabling technology and will be discussed in the following chapter. The following section first describes highlights in the history of the laser.

2.3 The History of the Laser

Historically, before the invention of microwave/molecular amplification by stimulated emission of radiation (maser) in 1953, usable and practical light emanated predominantly from spontaneous and scattered emissions from sources such as the incandescent bulb (first demonstrated in 1878) and other types of electromagnetic radiation such as IR, ultraviolet (UV) or gamma rays (Townes 1965). The maser was envisioned as a concentrated light source through research conducted by Charles H. Townes, Nikolay Basov and Alexander Prokhorov, leading to its invention in 1953. The maser is based on the theoretical principles of *stimulated emission* proposed by Albert Einstein in 1917, suggesting that excited atoms can radiate at specific wavelengths, including at visible light. To generate microwave energy for the maser, positive feedback by a resonant circuit is required to ensure that the gain in energy is greater than the circuit losses (Townes 1965). Masers are still used in various applications today, including satellite communication, radio telescopes, radar tracking, as oscillators in low-noise applications and as high-precision frequency references for atomic clocks. Masers, however, are historically associated with unwieldy machines requiring active cooling and producing small amounts of usable power as light. Maser research is still conducted; for example, in August 2012 Oxborrow et al. (2012) reported new interest in maser technology when scientists succeeded in exciting pentacene ($C_{22}H_{14}$) molecules by using a high-power laser and releasing microwave particles.

The maser is the predecessor of the laser. "A laser consists of an amplifying atomic medium occupying all or part of the volume of a suitable resonator. The role of the resonator is to maintain an electromagnetic field configuration whose losses are replenished by the amplifying medium through induced emission" (Yariv and Gordon 1963). In 1960, Theodore H. Maiman succeeded in operating the first pulsed ruby (chromium in corundum; Al_2O_3:Cr) laser. The original paper in August 1960 (Maiman 1960), a single-page article in Nature, reported that "an optical pumping technique was applied to a fluorescent solid resulting in the attainment of negative temperatures and stimulated optical emission at a wavelength of 6943 Å[1]" (694.3 nm). The first CW laser, a gas-based laser using helium (He) and neon, was demonstrated by the Iranian physicist Ali Javan in January 1961. The results are recorded in Javan et al. (1961).

[1]1000 angstroms (1000 Å) = 100 nanometres (100 nm).

During the 1960s researchers focused largely on the mechanisms to improve ruby-pulsed lasers and gas-based CW lasers. The US Army Electronics Research and Development Laboratory developed and demonstrated a ruby laser Q-switching technique involving the use of a revolving mirror mechanism, which generated single pulses of megawatt power, in August 1961. In Porto (1963) a technique to measure ruby laser outputs by reflecting the laser light in a barium sulfate ($BaSO_4$) diffuse reflector was presented and led to improvements to measure laser output wavelength. Bhawalkar et al. (1964) presented work on investigation of the spike pulses from the relaxation oscillator in a pulsed laser and Evtuhov and Neeland (1965) reported on measurement and interpretation of the frequency separation between transverse modes in ruby lasers. Military interest in using laser rangefinders was mentioned as early as 1965 (Benson and Mirarchi Benson and Mirarchi 1964) in a publication in which the limits to the range and accuracy of early lasers because of random and low-energy pulsed energy in these systems are addressed. The principle of the laser was already well-established in the 1960s and as seen from these early research papers, focus on its improvement received much attention from scientists. From the first pulsed ruby laser, many variations and different types of lasers have emerged, each with its own set of advantages, disadvantages and intriguing characteristics. Before discussing the types of lasers used in commercial, research and military applications and research, the basic principle of laser physics is presented.

2.4 The Basic Principles of Laser Physics

In the most general terms, a laser uses a mechanism that amplifies and guides light signals at a specific wavelength through a narrow and concentrated beam or cavity. Light is guided by either stimulated emissions or optical feedback, where oscillations of the light beam are typically provided by reflector mirrors. A simplified schematic representation of a laser system is given in Fig. 2.2.

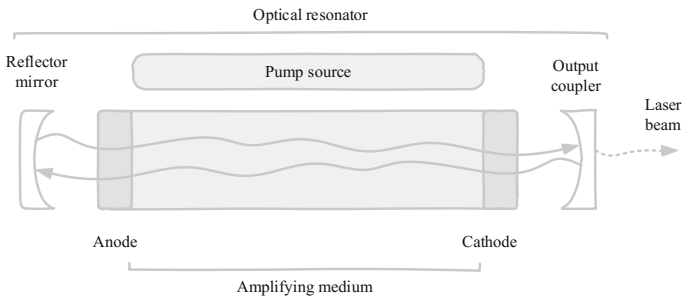

Fig. 2.2 Simplified representation of a laser system and the path of the light beam

As shown in Fig. 2.2, the laser consists of a gain or amplifying medium, also called the lasing material, to energize the light. The lasing material can be a crystal, gas, semiconductor or liquid dye and this is where stimulated emission occurs. A pump source, connected electrically by its anode and cathode, adds energy to the lasing material and the electrons that are added are excited to a higher energy level in a process known as population inversion. The process that induces population inversion in one form or another is called pumping. Pumping can be supplied by an electric current, by a light at a different wavelength than the generated output light or by another laser. Excited electrons then reside in an unstable condition and rapidly decay into its original energy state. The decay of these electrons occurs in two ways, either falling to its ground state while emitting randomly directed photons (light) or from spontaneously decaying electrons striking other excited electrons, causing them to descent to their ground state. The stimulated change releases energy as photons of light that travel at the same wavelength and phase as well as in the same course as the incident energies. Emitted photons move back and forth in an optical resonator and a set of mirrors feeds the light back into the amplifier to increase the developing beam in the optical cavity continuously. At the back of the laser is a fully reflecting mirror to ensure that the beam cannot escape the device at this end and in the front, a portion of the beam is emitted out of the device and a portion is reflected back into the loop through an output coupler. This systematic approach eliminates the possibility of the generated light radiating in all directions from the source and ensures that it has a focused trajectory in a single direction.

Optical amplification in the gain medium can be described by its energy level diagram, showing how the pump source induces transitions of ions from an excited state towards lower states. Quantum mechanical forces in atoms force electrons to take on discrete positions in orbitals around the atom nucleus. A simplified representation of the quantum mechanical effects that induce emission of light is given in Fig. 2.3.

Figure 2.3 shows the three distinguished states of a stimulated electron and the stages of spontaneous emission. If the electron is excited by an external source it takes on an excited state, depending on the energy applied to the system (ΔE). It therefore moves from a ground state E_1 to the excited state at E_2. The change in energy intensity is due to the incident photons directed at the material, such that

$$E_2 - E_1 = \Delta E = hv \tag{2.7}$$

where h is Planck's constant (4.135×10^{-15} eV s = 6.626×10^{-34} J s)[2] and v is the velocity of the incoming light. The energy added to the system can be either through incident photons (light) or incident heat/radiation (phonons) and the energy is transferred to the electrons, while in the excited energy state the electrons must naturally decay back to the ground state if the incident energy is removed or lowered. This fact highlights the reason why in 'pulsed' lasers, electrons are given a

[2] 1 Joule (1 J) = $6.242 \times 10^{+18}$ electron-volts ($6.242 \times 10^{+18}$ eV).

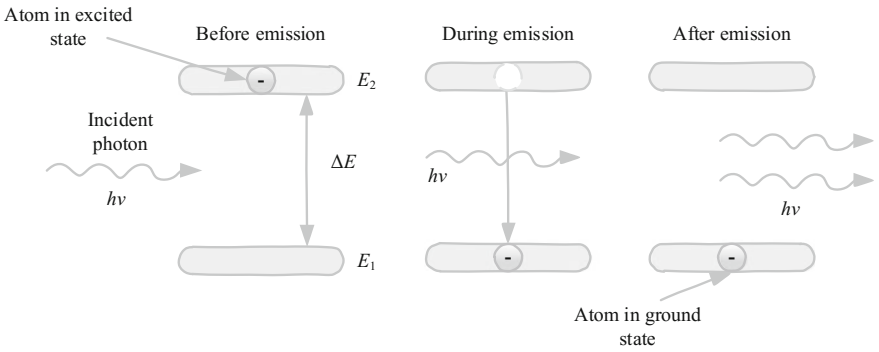

Fig. 2.3 Quantum mechanical effects showing the electron states before, during and after stimulated emission

fair chance/time to decay. During this stage, as the electrons decay, emission of light occurs with a wavelength dependent on the gas, solid or liquid material. The pulse of incident energy must be longer than the inherent time constant of the decaying transition to allow the electrons to reach the lower energy level. If the electron finds an unoccupied state in the lower energy level it emits a photon and this is called spontaneous emission. This photon again has an energy of hv and is spectrally defined at a wavelength. The photon exhibits random phase properties and multiple photons that are emitted without any phase relationship, therefore in random directions, are called fluorescence and thermal radiation—a random occurrence.

In Bäuerle (2013) the thermal and non-thermal processes (thermo-physical, thermochemical, photochemical and photo-physical[3]) of the excitation energy are described using the relaxation time τ_T (molecules moving from E_2 to E_1 in Fig. 2.3) and structural rearrangement time τ_R (molecules moving from E_1 to E_2 in Fig. 2.3) of atoms or molecules within the surface of the material. For a thermal laser process it should hold true that $\tau_T \ll \tau_R$ and a source must be used with $hv > E_g$ to excite electrons to a higher state. Laser-driven heat sources follow the same thermo-physical and thermochemical processes as conventional heat sources; a significant difference in these heat sources is the ability to induce temperature increases localized to small volumes in space and time by focused laser beams. Short and high-powered driver pulses add to thermal emissions through kinetic energy transfer as well.

Photochemical lasers operate under the condition that the thermal excitation energy time constant is relatively slow compared to the natural transition times, therefore when $\tau_T \geq \tau_R$. This process assumes that molecules are already absorbed in the top layer of the material and can interact and react with photolytic chemicals

[3]Photo-physical processes are defined as processes where thermal and non-thermal mechanisms contribute to the overall processing rate (Bäuerle 2013).

to transfer charge between states. Under a laser irradiation source these reactions typically show small variations in temperature over time. Bäuerle (2013) presents a model of the total reaction rate as the sum of the thermal channel (W_T) and the photochemical channel (W_{PC}) such that

$$W = W_T + W_{PC} = k_A \tilde{N}_A \left[1 + \frac{k_{A^*}}{k_A} \left(1 + \frac{h\nu}{\sigma I \tau_T} \right)^{-1} \right] \tag{2.8}$$

where A and A^* characterize the system in the ground state and excited state respectively, σ is the excitation cross-section, k_i is the rate constant of the system state (τ_i^{-1}), I is the intensity of the incident radiation and $\tilde{N}_i$ is the quasi-stationary density of species at its occupying state. The relevance of (2.8) is specifically found in its ability to characterize the process as thermal or photochemical through the time constant τ_T. For very small constants ($\tau_T \ll \tau_R$) the total reaction rate depends primarily on k_A and the thermal channel dominates. As the time constant rises in relation to the rearrangement time, the interaction and competition between thermal and photochemical processes become significant. The heat distribution of fixed laser parameters within the irradiated zone can be modelled by the heat equation, assuming the absence of thermal radiation and heat transport by convection. The heat equation in a Cartesian coordinate system that is fixed with the laser beam is given in Bäuerle (2013) through the first law of thermodynamics (conservation of energy) such that the spatial energy in the system $Q(x, t)$ is given by

$$\begin{aligned} \rho(T) c_p(T) \frac{\partial T(x,t)}{\partial t} - \nabla[\kappa(T) \nabla T(x,t)] \\ + \rho(T) c_p(T) v_s \nabla T(x,t) = Q(x,t) \end{aligned} \tag{2.9}$$

where $\rho(T)$ is the mass density and $c_p(T)$ is the specific heat at constant pressure, v_s is the velocity of the medium relative to the heat source and κ is the thermal conductivity. In the most general case $T \equiv Y(x, t) = T(x_a, t)$ is a function of both the spatial coordinates x_a and the time t (Bäuerle 2013).

To achieve stimulated emission and increase the probability of an atom entering a transition state called absorption where the incident photon is destroyed, an external electromagnetic field at a frequency associated with the transition is added to the system. Population inversion is essentially the redistribution of atomic energy levels in a system and what makes laser emissions occur. In a simple two-level energy system, it is not possible to obtain a population inversion with optical pumping, as the atoms in such a system are in thermal equilibrium and there are effectively more atoms in the lower energy state than in the higher energy state. If atoms in a two-level energy system are excited from the ground state to the excited state, statistical equilibrium will eventually be reached in response to spontaneous and stimulated emissions. Equal population of the two states can be achieved, which results in optical transparency but without remaining optical gain. To achieve non-equilibrium conditions, an indirect method of populating the excited state must

be used. The minimum pumping power ($P_{\min}$) for a pumping process that is assumed to be 100 % efficient, i.e. only the energy lost by radiation needs to be replenished, can be determined by

$$P_{\min} = \frac{N_m hc}{\lambda_L t_c} \tag{2.10}$$

where N_m are the finite number of modes of the laser within its finite bandwidth, the energy in the given mode is characterized by the average lifetime t_c and the operation wavelength is given by λ_L. The rate of stimulated emission is proportional to the difference in the number of atoms in the excited state (N_2) and in the ground state (N_1), which depends on the average lifetime of the atoms in the excited state and the average lifetime of the emission in the laser cavity. Mathematically this is represented by

$$\Delta N_m = N_2 - N_1 = \frac{N_m \tau}{t_c} \tag{2.11}$$

where the atoms with an excited state have a lifetime of τ if placed inside a cavity. For an electron bound to a nucleus and residing at an atomic orbital, its energy level is related to its state by

$$E_m = -hcR_\infty \frac{Z^2}{N_m^2} \tag{2.12}$$

where R_∞ is the Rydberg constant ($R_\infty = 1.097 \times 10^7$ m^{-1} and $hcR_\infty = 13.605$ eV) and Z is the atomic number. If there are more atoms in the upper level than in the lower level, the system is not in equilibrium and the distribution of atoms between the levels is given by Boltzmann's law as

$$N_2 = N_1 x e^{\left(\frac{E_2 - E_1}{kT}\right)} \tag{2.13}$$

and in this case, N_2 is always less than N_1. To create a situation where atoms are not in equilibrium, an external factor is required to vary the energy levels between states. In lasers, this is called the pumping stage (electrical, optical or chemical), raising atoms to an excited, upper energy level. Light can only be amplified if $N_2 - N_1 > 0$. In optical pumping there must be at least three distinct energy levels to create a population inversion. The energy-level diagram of a three-level system is given in Fig. 2.4.

Figure 2.4 shows the pumping transition between E_1 and E_3 and laser transition as the atoms decay from E_2 and E_1. The transition between E_3 and E_2 is a rapid decay from the highest energy state to the metastable energy level but does not contribute to laser radiation. This transition between E_3 and E_2 limits the possible systems that allow population inversion in three-level systems. Although this representation of energy transitions seems simple to achieve, the ground state of the

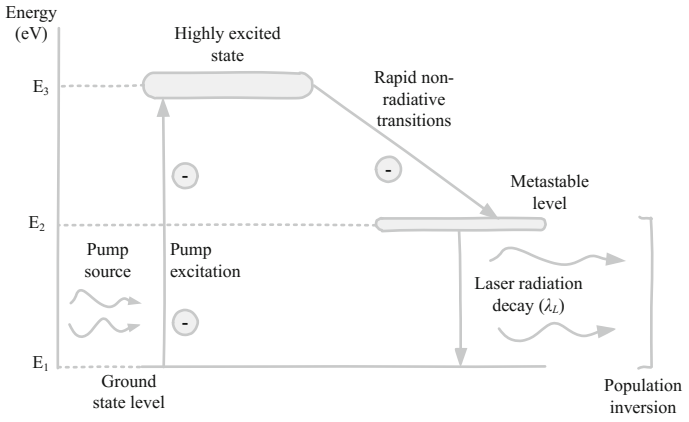

Fig. 2.4 Energy level diagram showing the principle of a three-level system

energy system has a large population of atoms at thermodynamic equilibrium. The practical implementation of achieving such a system is more complex and requires high-powered pumping energies. The metastable energy level (E_2) must be able to store atoms decaying from E_3 and ensure that spontaneous non-radiative emissions become less likely. It also requires great pumping energy to excite atoms from E_1 to E_3. The first ruby laser demonstrated in 1960 used Al_2O_3:Cr, an aluminum crystal matrix doped with Cr^{3+}, whose energy levels match such a three-level system and create the laser effect.

Another example of a spectroscopic system is the four-level laser. The four-level system is depicted in Fig. 2.5.

In the four-level system in Fig. 2.5 the optical pumping transition and the laser transition occur over a pair of distinct levels (E_1 to E_4 for the pumping and E_2 to E_3 for the laser transition). E_2 is chosen to be sufficiently far away from the ground state E_1 to ensure that the thermal equilibrium at thermodynamic equilibrium is negligible. Atoms do not stay in E_4 or E_2 and atoms excited to E_4 rapidly decay to E_3 with non-radiative emissions and from E_2 to E_1 due to natural depopulation, also a non-radiative transition. As soon as an atom moves to E_3, a population inversion occurs and the medium becomes amplifying. To maintain the population inversion, atoms should not accumulate in E_2, but must rapidly decay to E_1. A known compound commonly used that operates as a four-level energy-level system is neodymium YAG, given by $Nd:Y_3Al_5O_{12}$, and emanates at a wavelength of 1064 nm.

An example of a spectroscopic system using an electrical pumping mechanism and energy transitions is a He-neon (HeNe) gas system. Such a system is depicted in Fig. 2.6.

In the HeNe system shown in Fig. 2.6 the neon transitions are used for the laser transitions and He is the intermediary gas capable of transferring energy from the electrons to the neon particles through collisions. It should be noted from Fig. 2.6

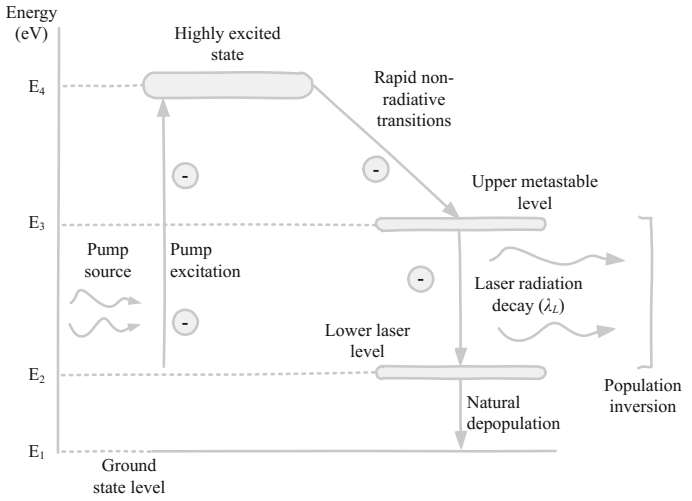

Fig. 2.5 Energy level diagram showing the principle of a four-level system

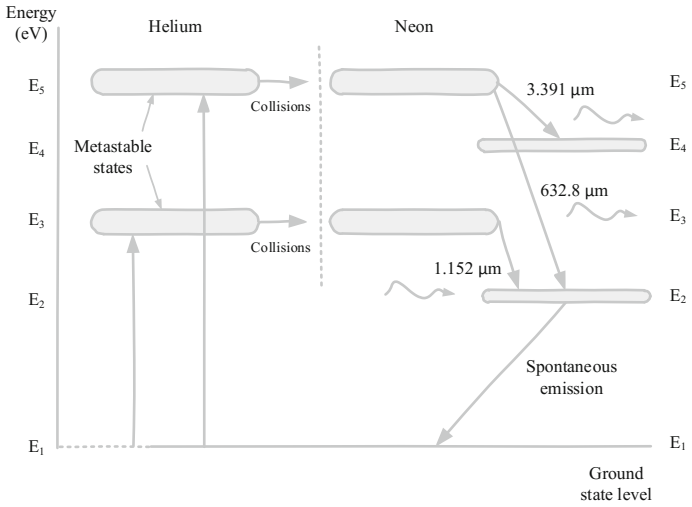

Fig. 2.6 Energy level diagram of a HeNe gas system using electrical pumping to transition between states

that the lower levels of the laser transitions occur relatively far from the ground state and this favors population inversion as opposed to thermal population. He has an additional characteristic in that it has two metastable states where atoms can stay for longer periods of time before falling to the ground state. He atoms are transported to the excited state through collision with electrons. Energy is transferred to

the neon particles when the atoms collide because these metastable levels of He coincide with the excited states of the neon. The process of population inversion can simplistically be represented by

$$\mathrm{He}^{*} + \mathrm{Ne} = \mathrm{He} + \mathrm{Ne}^{*} \tag{2.14}$$

where He^{*} and Ne^{*} represent the atoms at excited levels. The transfer of energy occurs while atoms decay to lower energy levels. HeNe systems can emit radiative laser light at 543, 632.8, 1152, 1523 and 3391 nm; 632.8 nm radiation is most commonly used in commercial applications such as optical laser-disc readers. A list of commonly used laser materials with various energy-level systems and their corresponding wavelengths and applications are given in Table 2.3.

The optical power output of a laser is dependent on the in-lasing threshold. This threshold is the lowest excitation level at which the output is dominated by stimulated emission as opposed to spontaneous emission. This depends heavily on the material used and its band gap (discussed in more detail in the following section). The optical power output of a laser beam is its continuous power output of CW lasers or the average power for a pulsed laser. The energy of a laser (E_{laser}) is the output of a pulsed laser and is related to the maximum attainable power output (P_{pk}), where

$$E_{laser} = P_{pk} \times t \tag{2.15}$$

where t is the duration of the laser pulse in seconds. The average power (P_{avg}) of a pulsed laser is the pulse energy multiplied by the frequency (f) of the laser repetitions per second, such that

$$P_{avg} = E_{laser} \times f. \tag{2.16}$$

Therefore, at constant average power levels, short pulse lengths (pico- to femtoseconds) result in high peak output powers with relatively low pulse energy, whereas long pulse lengths (milliseconds) result in low peak power but high pulse energy.

In Marshall and Burk (1986) the parameters to determine the optical link performance between a transmitter and a receiver through an optical channel are described. In this article the detector sensitivity and required signal calculations are not considered in the optical link performance and are determined purely from analytic models of the system components concerning the laser. The link parameters are listed in Marshall and Burk (1986) as part of a block diagram of an optical communications transceiver consisting of a laser, communications detector, optical assembly and a receiving telescope (optics) and are adapted and given as

- laser average output power (P_{avg}),
- laser wavelength (λ),
- transmit telescope aperture diameter (D_t),
- transmit telescope obscuration ratio (γ_t),

Table 2.3 Commonly used laser materials and their formulas, emitted wavelengths and example applications

Laser material	Formula	Wavelength (λ_L) in nm	Applications
Alexandrite (chrysoberyl)	$BeAl_2O_4$	755	Laser hair removal
Argon		457–528	Photocoagulation in ophthalmology, limited lifetime applications
Argon fluoride (exciplex)	ArF	193	IC production (photolithography), eye surgery
Carbon dioxide	CO_2	10,600	High-power CW applications, cutting, welding, engraving, military range-finding, LIDAR
Carbon monoxide	CO	5000–6000	Glass, metal and ceramic processing, skin resurfacing, surgical cutting
Copper vapor	CVL	510.6/578.2	Analytical instruments, spectroscopy
Erbium:Glass	(CR14 or EAT14)	1540	Skin resurfacing, optical fiber communication
Frequency doubled Nd:YAG	see Nd:YAG	532	Ophthalmology, oncology, laser peeling, laser rangefinders and designators
Helium cadmium	HeCd	325 (UV)/ 442 (blue)	Spectroscopy, stereo lithography
Helium neon	HeNe	632.8 (most used)	Laser disc players, laser alignment, particle measurement, velocimetry
Hydrogen fluoride	HF	2700–2900	High-power CW applications (military and space—missile defense)
Krypton fluoride	KrF	337.5–799.3	Photolithography
Laser diodes	–	405–950	Fiber-optic communication, DVD/Blu-ray readers, laser printing/scanning, laser pointers
Nd:YAG	$Nd:Y_3Al_5O_{12}$	1064	Laser-induced thermotherapy, scientific research
Rhodamine 6G	$C_{28}H_{31}N_2OCl$	450–650	Dye lasers, tunable lasers[a] (wide bandwidth research applications)
Ruby	Al_2O_3:Cr	694.3	Laser range-finding, holographic portraits, hair removal, tattoos
Ti:Sapphire	$Ti:Al_2O_3$	690–1100	Scientific research (due to tenability and ultrashort pulses)
Xenon fluoride	XeF	351	Photolithography, micro-machine plastics and composites
Xenon monochloride	XeCl	308	Dermatology, micro-machine organic tissue, precision surgery

[a]Coldren et al. (2004)

- transmitter optics throughput (η_t),
- transmitter pointing bias error (ε_t),
- transmitter jitter (σ_t),
- receiver telescope aperture diameter (D_r),
- receiver telescope obscuration ratio (γ_r),
- receiver optics throughput (η_r),
- narrowband filter transmission (η_λ),
- receiver point bias error (ε_r),
- receiver jitter (σ_r),
- narrowband filter spectral bandwidth ($\Delta\lambda$), and
- detector diametrical field of view (θ).

From the parameters listed above the transmitter and receiver optics throughput, transmitter and receiver pointing bias error and jitter, the receiver telescope aperture diameter and the receiver telescope obscuration ratio can be calculated from the reflection and transmission coefficients of the components in the optical system. Marshall and Burk (1986) state that to determine the link performance accurately, the system operational parameters must also be defined. These parameters include the

- data rate R,
- pulse-position modulation (PPM) alphabet size M,
- PPM slot time τ_s,
- link range L,
- atmospheric transmission loss factor $L_{a,}$ and
- background radiance B.

A convenient method to determine the number of received signal photons per PPM word for a laser pulse N_S as a normalized value of received power P_r in watts and the PPM word rate is presented in Marshall and Burk (1986) as

$$N_S = P_r \frac{\log_2 M}{R} \frac{\lambda}{hc}. \tag{2.17}$$

It follows that the number of received background photons per PPM slot time is given by

$$N_B = P_B \tau_S \frac{\lambda}{hc} \tag{2.18}$$

where the collected background power from point sources such as stars and extended sources such as scattered light is given by P_B and represented as

$$P_B = BL_a \frac{\pi D_r^2}{4} \left(1 - \gamma_r^2\right) \frac{\pi \theta^2}{4} \Delta\lambda \eta_r \eta_\lambda. \tag{2.19}$$

The equations to determine the number of photons per laser pulse assume that the type of laser and therefore the wavelength of the operation are known. The following section highlights the types of lasers used in commercial, research and military applications and the differences in operating modes between the types. Types of lasers including gas, chemical, liquid dye, metal-vapor, solid-state and semiconductor lasers are presented and discussed with precedence given to semiconductor lasers, since the context of this book is predominantly aimed at semiconductors and microelectronic technologies. SiGe can be used as lasers emitting in the THz spectral range (Kelsall and Soref 2003) and the technology is present in fast-switching electronic support circuitry and laser drivers (Knochenhauer et al. 2009 and Moto et al. 2013) discussed in the following chapter. Electroluminescence signals observed from the intersubband transitions in SiGe heterostructure quantum-cascade (QC) lasers have only been realized in the past decade and applications such as free-space communication within the atmospheric window and detection and trace analysis of organic metals (Tsujino et al. 2006) are among the primary fields that can benefit from this technology. Semiconductor lasers are only one category of several types of lasers and these types are discussed below to distinguish between the various alternatives.

2.5 Types of Lasers

Lasers operate on the principle of guided luminescence as a result of stimulation of a material and specifically exclude the luminescence resulting from the temperature (radiation) of the material (Ivey 1966). Luminescence may occur in gaseous, liquid or solid materials; solids offer the most practical means of implementation, primarily owing to the containment methods of the material. The three main categories of laser types are further divided into sub-categories, as shown in Fig. 2.7.

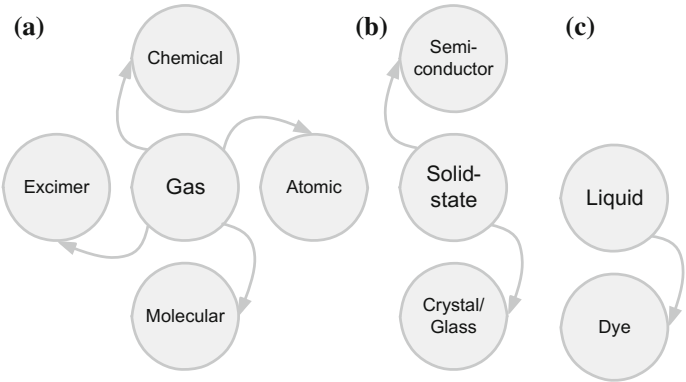

Fig. 2.7 Three main categories of lasers **a** gas, **b** solid-state and **c** liquid lasers and sub-categories of each

In Fig. 2.7 the three main categories of laser types are given, these being gas, solid-state and liquid lasers. Figure 2.8 distinguishes further between some of the most well-known examples of each type of laser.

Types of luminescence are distinguished based on the source of input excitation energy (photoluminescence, cathode luminescence and electroluminescence). Photoluminescence occurs in response to optical radiation, cathode-luminescence is generated by electron beams in cathode rays and electroluminescence is generated by electric fields or currents applied to the material. The source of the excitation process can differ; however, the physics of the transitions as a result of excitation remains the same across excitation methods. Adapted from Ivey (1966), there are three main categories of emitting transitions, which depend on the material and the conditions. These categories are defined by Ivey (1966) as

- transitions involving chemical impurities or physical defects (conduction band to acceptor, donor to valence band or donor to acceptor),
- inter-band transitions (intrinsic emission corresponding in energy to the band gap and higher energy emissions involving hot carriers, also called avalanche emissions), or
- intra-band transitions involving hot carriers (also called deceleration emissions).

It should also be recalled that not all electronic transitions are radiative and are reliant on the radiative qualities of the material. Electroluminescence of semiconductors are generally spontaneous and random, giving incoherent radiation. Emissions of photons initiated by source photons occurs in phase with the stimulating source to generate coherent emissions. For coherent emissions the number of electronic states available for emission must exceed the number of states available for absorption (population inversion of active states). Optical gain is achieved if the stimulated emissions can overcome the optical losses in the material. Radiative semiconductors take advantage of its inherently high index of refraction to reflect light generated inside the material to follow a cavity or optical path naturally. If oscillations in the material take place in response to optical gain, the radiated light

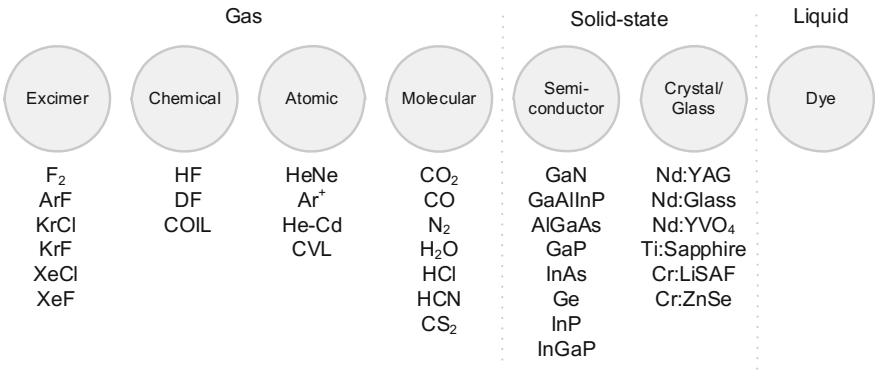

Fig. 2.8 Sub-categories of the types of lasers and common examples of each

will demonstrate spectral narrowing, phase coherence and beam directivity. The earliest recorded laser experiments were achieved in the early 1960s by injecting carriers in a forward-biased *p*-*n* junction using the direct band gap material GaAs (Nathan et al. 1962; Quist et al. 1962). GaAs was considered the most efficient and most common material used to conduct initial semiconductor laser experiments. Following the experiments conducted on GaAs, Bell Laboratories started researching phase chemistry and liquid epitaxy of $Al_xGa_{1-x}As$ injection lasers. A structure consisting of a layer of GaAs between *n*-type and *p*-type layers of $Al_xGa_{1-x}As$ showed simultaneous characteristics of acting as an optical waveguide and as a confinement region for the carriers injected in the GaAs laser in forward-biased conditions (Patel 1984). This led to the first room-temperature CW semiconductor laser at 880 nm in 1970 (Silfvast 2004). The following sections describe the operation principle of semiconductor lasers, solid-state, gas, chemical and liquid dye lasers in varied degrees of detail. Semiconductor lasers are used as the reference benchmark to elaborate further on the principles of laser operations since solid-state, gas, chemical and liquid dye lasers share many of their operating principles where primarily the pumping method and optical gain differ.

2.5.1 Semiconductor Lasers

Semiconductor lasers operate on the principle of semiconductor gain media, a condition induced by stimulated emission at an interband transition when the conduction band is at a higher carrier density. The gain in a semiconductor is a phenomenon where photon energy above the semiconductor band gap energy can excite electrons into a higher state in the conduction band. As the electrons reach this higher energy level they rapidly decay to states near the bottom of the conduction band. During this period, holes generated in the valence band move to the top of the valence band and electrons in the conduction band can recombine with these holes. During this recombination, photons are emitted at an energy near the band gap energy of the semiconductor. The energetic bands mentioned in the description of gain media above are classified as empty, filled, mixed or forbidden in semiconductor physics. Figure 2.9 depicts the band structures for insulators, semiconductors and conductors (metals).

The energy levels in Fig. 2.9 are occupied by electrons, starting at the lowest energy level. Electrons contributing to electronic conduction are situated in the higher energy bands. Electrons occupying the highest energy band in equilibrium are known to exist within the valence band. The insulator energy band structure in Fig. 2.9 indicates that the energy separation between the valence and conduction band is the largest and these materials do not conduct electrons under normal circumstances. Semiconductors have a smaller band gap between the valence and conduction bands and by applying an energy (electric field) higher that the band gap to the anode and cathode of the material initiates conduction of the material. In conductors such as metal, the conduction band and valence band overlap and there

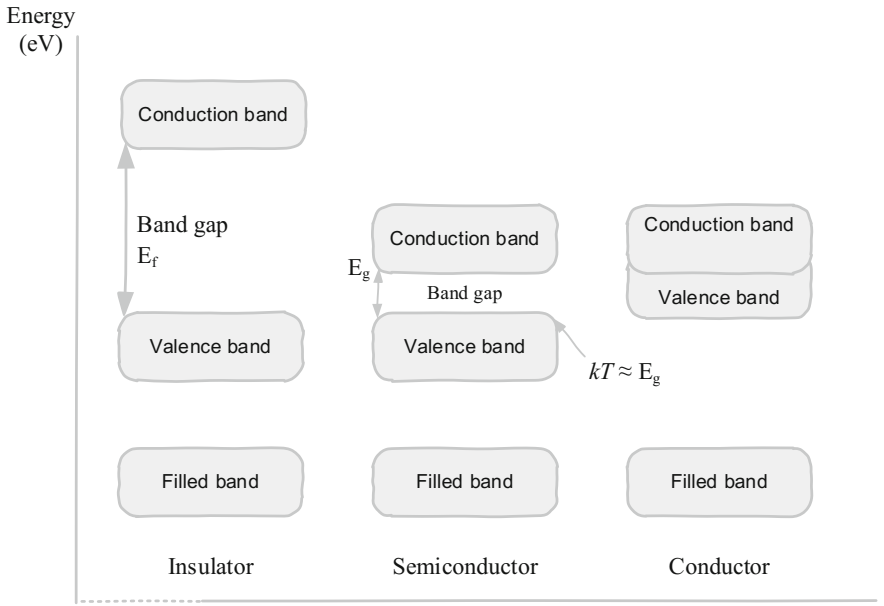

Fig. 2.9 Energy band structure of solid insulators (non-conducting materials), semiconductors and conductors (metal)

is no band gap between these energy levels. These materials conduct electrons under normal circumstances.

In semiconductor lasers the external energy to excite the electrons to higher states are applied by means of an electric field across its p and n junctions. If the electric field is applied, the electrons in the semiconductor structure acquire directed velocities in the opposite direction of the applied electric field. Each electron has momentum of

$$p = m^* v \tag{2.20}$$

where m^* is the effective mass of the electron moving in the lattice and having a different mass compared to a free electron due to its additional kinetic energy E (and its effective mass may also be negative—Einstein 1905). To relate the momentum, p, of the electron to its wavelength, the Broglie relation of

$$p = \frac{h}{\lambda} \tag{2.21}$$

can be used where h is Planck's constant and λ is the wavelength. The momentum, kinetic energy and the wave vector **k** can be related by

$$E = \frac{1}{2}m^* v^2 = \frac{p^2}{2m^*}. \tag{2.22}$$

It is shown in Gilmore (2004) that in momentum conservation the wave-function

$$\Phi_1(x) = e^{+ikx} \tag{2.23}$$

represents a particle to the right of a region with constant potential (electric field) $V < E$ with a specific momentum and if

$$k = \sqrt{2m(E - V)/\hbar^2} \tag{2.24}$$

and the reduced Planck constant $\hbar$ is given by

$$\hbar = \frac{h}{2\pi} \tag{2.25}$$

and

$$p = \hbar k \tag{2.26}$$

then (2.22) can be rewritten as

$$E = \frac{\hbar^2 k^2}{2m^*} \tag{2.27}$$

used to draw the energy bands as parabolas on an *E-k* diagram. The *E-k* diagram (see Fig. 2.10) shows the relationship between the energy and momentum of available quantum mechanical states for electrons in a material. In semiconductor materials it shows the band gap of the material, which is the difference in energy between the top valence band and the bottom conduction band and the effective mass of holes and electrons in the material through the curvature of each band in the diagram. It also indicates how the electron states are equally spaced in the *k*-space —in essence showing the density of states depending on the slope of the curve.

Semiconductors can be classified as direct band gap or indirect band gap materials. Defining the band gap for semiconductors is important in determining physical properties such as photoconductivity (photodetectors) and electroluminescence (lasers).

Semiconductors that can emit photons (crucial for laser operation) fall in the direct band gap category, since the crystal momentum of the electrons and holes is the same in the conduction and valence band. This means that an electron in the lowest-energy state in the conduction band can shift towards the highest-energy state in the valence band with zero change in crystal momentum.

In an indirect band gap semiconductor, the electron must first pass through an intermediate state and transfer momentum to the crystal lattice; photons are not

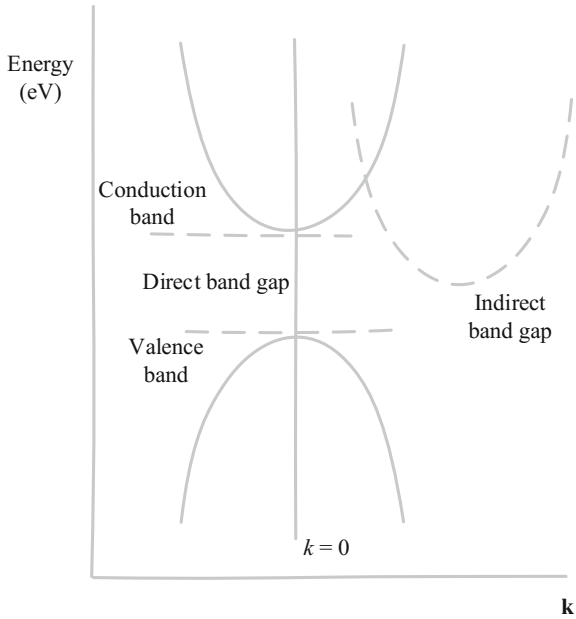

Fig. 2.10 Direct and indirect band gaps and the **k**-vector; showing the change in momentum for indirect band gap solid materials that cannot emit photons freely (adapted from Seo and Hoffman 1999)

likely to be emitted from the lattice. The crystal momentum responsible for the photon emission is described by the **k**-vector in the Brillouin zone defined as the plane boundaries of reciprocal lattice structures. Interactions between electrons, holes, photons and phonons must fulfil the conservation of the energy theorem and crystal momentum principles—thus the conservation of the total **k**-vector (Seo and Hoffman 1999). A photon with energy near the semiconductor band gap has close to zero momentum. Models used to describe free-carrier dynamics in the conduction band include the Boltzmann equation, the Fokker-Planck equation, Monte-Carlo methods, Stuart's single rate equation for the free-electron density and the multi-rate equation model (Gulley 2011). The direct and indirect band gap structures and the **k**-vector are depicted in Fig. 2.10 (Seo and Hoffman 1999).

There are various methods to determine if a solid semiconductor material has a direct or indirect band gap. These methods include plotting the optical absorption coefficient with varied wavelengths, spectroscopy, the *Tauc* plot (Tauc 1968) to determine direct/indirect and allowed/forbidden transitions and the shapes of the highest occupied molecular orbital and the lowest unoccupied molecular orbitals of constituent monomeric conjugated organic molecules.

In principle, a semiconductor/diode laser can be manufactured from any type of direct band gap material, but the efficiency of electrically injected lasers is dependent on precise doping concentrations of the active layers and require lattice-matched materials to facilitate molecule interaction between layers. Most commercial lasers used in for example pumping fiber amplifiers in telecommunications use III-IV compounds such as GaAs and InP heterojunction

semiconductors. These materials present good lattice matching and efficient transport. Longer wavelengths of up to approximately 10 μm require other materials such as antimonide (Sb) as an alloy; for smaller wavelengths in the near-UV band (approximately 400 nm) epitaxial layers such as GaN are used. Defense and security applications often use vertical stacked lasers manufactured in II-IV compounds (ZnSe and ZnS for example) with light intensities of up to 2 kW (Laser Enterprise 2016). Common materials used in semiconductor lasers and for other optoelectronic devices are listed in Table 2.4.

Table 2.4 gives an indication of the wavelength of the laser light when implemented in various semiconductor materials. The equation used that relates the bandgap (E_g) and the cut-off wavelength (λ_{co}) is given by

$$\lambda_{co} = \frac{hc}{E_{g,}(eV)} \tag{2.28}$$

where h is Planck's constant and c is the speed of light in free space in m/s. In ternary and quaternary semiconductor compounds such as $Al_xGa_{1-x}As$ as in Table 2.4, the band gap can be varied by changing the content of the materials. The content of the material is defined by x where $1 \leq x \leq 0$. Another example in Table 2.4 is $In_xGa_{1-x}As$, where if $x = 0.53$ then the compound is defined as $In_{0.53}Ga_{0.47}As$ with $E_{g,300}$ of 0.75 eV.

Variant configurations of semiconductor layers produce different laser types; these include single-spatial-mode, multimode, bars and stacks, single-mode distributed feedback (DFB) and less commonly used lasers such as vertical cavity surface-emitting lasers (VCELs), distributed Bragg reflectors (DBRs) and tunable DFB lasers.

The simplest form and also the most commonly used one in commercial lasers is the single-spatial-mode laser. It is also called the single transverse mode laser

Table 2.4 Energy band gap and cut-off wavelengths of commonly used materials in semiconductor direct band gap lasers defined at 300 K

Material	Symbol	$E_{g,300}$ (eV)	λ_{co} (nm)	Band
Aluminium gallium arsenide	$Al_xGa_{1-x}As$	1.42–2.16	575–875	Visible
Gallium arsenide	GaAs	1.42	875	Visible
Gallium nitride	GaN	3.4	365	Near UV
Gallium phosphide	GaP	2.26	555	Visible
Germanium	Ge	0.66	1800	Short IR
Indium antimonide	InSb	0.17	5700	Medium IR
Indium arsenide	InAs	0.36	3400	Medium IR
Indium gallium arsenide	$In_xGa_{1-x}As$	0.73–0.47	1700–2600	Short IR
Indium gallium arsenide	$In_{0.53}Ga_{0.47}As$	0.75	1 655	Short IR
Indium gallium phosphide	InGaP	1.90	655	Visible
Indium phosphide	InP	1.35	919	Near IR

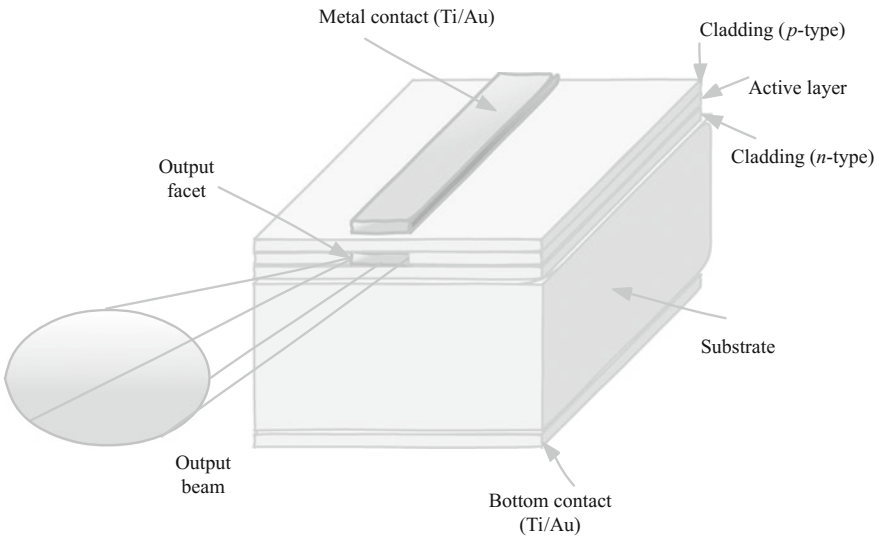

Fig. 2.11 Representation of a double-heterostructure single-transverse-mode semiconductor laser configuration

because of the implication that the beam can be focused to a diffraction-limited spot. Figure 2.11 shows a typical single-spatial-mode laser with a relatively narrow waveguide bounded by cleaved facets (Photonics Handbook 2015).

The single-spatial-mode laser in Fig. 2.11 shows a heterostructure with a narrow waveguide to guide the output laser beam. This waveguide can be achieved by a ridge-structure or a buried index step during processing. A single optical mode is supported in such a structure. The width of the waveguide is typically limited to 2–5 μm, depending on the actual waveguide structure. At the output facet the emitted laser light is typically around 1 μm high and 3–4 μm wide—again depending on the actual structure and application (Photonics Handbook 2015). As the laser light leaves the output facet, it naturally diverges into vertical and horizontal directions. The vertical divergence is perpendicular to the junction plane; it typically diverges about 20–30° and is referred to as the fast axis. The horizontal divergence is approximately 5–10° and called the slow axis. Since the divergence in the two planes is different (anamorphic), the output beam forms an oval shape. The output beam can also be somewhat astigmatic,[4] but both of these effects can be corrected through optics. Single-spatial-mode lasers are ideal when a diffraction-limited focus point is required, such as in optical data storage, thermal printing, fiber communications and laser pointers. Maximum average power output is limited in these lasers by the narrow waveguide generating significant local power density and

[4]Astigmatism in an optical system is when the rays propagating in two perpendicular planes have different focus points.

thermal dissipation. Trading off spatial coherence, to increase the average power output, the width of the waveguide can be increased to several hundreds of microns. These lasers are called broad-area or multimode lasers.

Multimode lasers cannot be focused to a diffraction-limited spot or efficiently coupled into a single-mode fiber (Photonics Handbook 2015). The output power also does not increase proportionally with the increase in the width of the waveguide. Applications that do not require diffraction-limited focus include external-drum thermal printing techniques and pumping solid-state lasers using high average output power (up to 6 watts at the expense of spatial coherence). To achieve even higher average output power in the order of 100 W, bars and stacks of multimode lasers are combined in a single structure and optically corrected at the output. Bar dimensions can be in the order of 1 cm high and 0.5–2 cm wide and a single bar can emit between 20 and 60 W of output power in CW mode and up to a 100 W in pulsed mode. Applications for high-powered pumping solid-state lasers at commercial wavelengths (785, 792, 808, 915 and 940 nm) typically use these configurations. To increase power further, bars are stacked in series and can thus use the same input voltage requirements with matched output impedance to the driver electronics; however, these configurations generally use large and costly high-current sources. These bar-stacked lasers are actively cooled (mostly water-cooled) during operation as a result of their high-current usage, can be used with or without optics depending on the application, found in applications for material processing where high beam quality is not required (welding, hardening, alloying or cladding of metals) and extremely high-power solid-state lasers. Single-mode DFB lasers offer low noise and narrow frequency spectrum characteristics and are becoming more common in optical transmission systems.

DFB lasers do not rely on mirrors to provide optical feedback; they use corrugated structures such as gratings close to the waveguide in the epitaxial layers. Each ripple in the grating offers a small amount of internal feedback and since the device uses a single frequency, each feedback from the gratings adds up in phase, which naturally decreases partition noise found when longitudinal modes in multi-frequency lasers interfere with each other. Noise levels of −150 dB/Hz are commonly seen in these DFB lasers. Applications in fiber-optic transmission systems requiring lower power but also very low-noise characteristics use DFB lasers to match high gain-bandwidth products (GBPs) of fiber amplifiers. DFB lasers are also found in interferometric and spectroscopic applications and have been demonstrated at wavelengths from 633 nm to upwards of 2000 nm. Other less common laser structures include VCEL, DBR and tunable DFB lasers.

In VCSELs, light propagates perpendicularly to the wafer and is emitted from its surface. To implement the required mirrors for optical feedback, mirrors are grown as multilayer dielectric stacks above and below the quantum well active layer.

> VCSEL multilayer stacks must have reflectivity as high as 99.8 % and the layer thicknesses must be precisely controlled to ensure that the resonator frequency falls within the gain bandwidth of the quantum well (Photonics Handbook 2015).

The growing and manufacturing of these devices are simpler compared to more traditional lasers and can be tested at wafer level, therefore making them more cost-effective and easier to control in terms of the quality and yield of the devices. VCSELs have low divergence and nearly circular beam profiles and are ideally used for coupling to optical fibers. DBR lasers provide a higher CW output power compared to DFBs at the cost of introducing mode hops with the drive current (Photonics Handbook 2015). Tunable DFBs can be achieved by having multiple grating structures introduced into the semiconductor, giving it a discrete tunable range, although increasing the manufacturing cost.

2.5.2 Solid-State Lasers

Semiconductor lasers also fall into the category of solid-state lasers (Figs. 2.7 and 2.8), but another type of solid-state laser is based on crystals or glass doped with rare earth or transition metal ions for the gain media. Another term for solid-state lasers, which specifically exclude semiconductor lasers, is doped insulator lasers. These can be manufactured in the form of bulk lasers, fiber lasers or other types of waveguide lasers. Commonly used solid-state lasers are mostly optically pumped with flash lamps or arc lamps and can achieve relatively high powers of tens of kilowatts. Drawbacks of solid-state lasers include low efficiency coupled with high thermal losses in the gain medium. As a result of the low efficiency and moderate lifetime due to thermal heating, laser diodes are often used for pumping solid-state lasers and actively cooled. These systems are called DPSS lasers and provide a good beam quality and better lifetime and are relatively compact systems.

Solid-state lasers present long lifetimes of radiative upper-state transitions, leading to efficient energy storage. This characteristic of solid-state lasers makes them suitable for *Q*-switching lasers that have extremely high peak powers. Solid-state lasers are generally not associated with large tuning bandwidths; rare-earth-doped laser crystals present a low tuning range, whereas rare-earth-doped glass lasers present a larger tuning range.

2.5.3 Gas Lasers

A gas laser is identified by the fact that the gain medium in the laser system is a gas that can be pumped by an electric discharge, RF waves, photons or e-beams. The gain medium consists of a narrow tube filled with a combination of gases (for example He and Ne). At its ends, an anode a cathode facilitates a high-current discharge through the tube, while mirrors at the ends of the tube provide optical feedback. Electrons from the discharge collide with the abundant gas atoms and excite these atoms to an upper metastable energy level. Through further resonant impacts the energy is transferred to the minority gas particles and raises these atoms

to nearly identical energy levels. These minority particles can then decay back to the ground state to facilitate population inversion. Particles generally follow different routes towards the ground state and as a result of these different paths also generate various wavelengths during radiation emissions. Rare-gas ion lasers achieve stimulated emission when the discharge current is high enough to ionize the gas and through the electron-ion interactions excite the ions from the ground state to the metastable states.

At IR wavelengths it is possible to achieve high-power lasers from molecular gas such as CO_2. These lasers generate stimulated emissions from the low-energy transitions between vibration and rotation states of molecular bonds. High-powered molecular lasers are generally used in electrically discharged pumping techniques but can use RF excitations as well. According to Endo and Walter (2006), some advantages of gas lasers are the ability of the gas to adopt the cavity shape quickly, scalability, long lifetime if in a high-quality vacuum, recyclability of gas, homogeneity, stability, possible use of isotopes to shift the radiation spectrum and the wide spectra covered by varying gas types.

Metal vapor lasers are also gas lasers that vaporize metal (such as copper) at high temperatures and use this vapor as the gain medium in an optical cavity. The high temperatures required to vaporize the metal make it difficult to implement metal vapor lasers practically and require the optical cavity and mirrors to withstand high temperatures. Materials other from pure copper, such as copper nitrate or copper acetylacetonate, can help to achieve lower temperature operation and make these systems realizable at lower cost and with increased modularity. Typically, to achieve population inversion in metal vapor lasers, two successive energy pulses are required to dissociate vapor molecules, followed by a pulse to cause the dissociated ions to lase. There are two main types of metal vapor lasers: ionized metal (such as He-Cd) and neutral metal (such as Cu) vapor lasers; both operate by vaporizing metal in a container.

2.5.4 Chemical Lasers

Chemical lasers use chemical reactions as opposed to light or electrical sources as the pumping source. The COIL laser presents high efficiency and high average power and has proved to be an important laser in antimissile defense systems. A major advantage of chemical lasers is the relatively small power generation required, which is a valuable commodity on mobile air defense systems such as missiles to initiate a chemical reaction. Most of the energy required for the lasing action is stored in the fuel/chemicals themselves. The basic principle of the COIL laser is therefore that a fuel such as Cl_2 gas is mixed with an oxidizing agent such as hydrogen peroxide (H_2O_2) in a combustion chamber and a spark is ignited to activate the reaction. The product of this reaction is the excited molecular oxygen. This reaction is mixed with an iodine vapor and flashed through a nozzle where the components interact to produce excited iodine atoms. The lasing activity is

achieved in an optical cavity across the expansion chamber. For atmospheric aerial applications, an iodine laser is ideal, since its 1300 nm wavelength falls in the atmospheric transmission window. For space-based applications, for example, HF lasers are considered to be more efficient.

2.5.5 Liquid Dye Lasers

The gain medium of liquid lasers is optically pumped liquids, typically at room temperature. The most common liquid lasers are dye lasers, which consist of organic dyes in liquid solvents. Dye lasers can generate a large bandwidth of laser light from the excited states of these dissolved dyes. The output types of these lasers can be either pulsed or CW and span across spectra from near-UV to near-IR, depending on the dye used (LaserFocusWorld 1995). The principal operation of dye lasers involves optically pumping the organic molecules to excited states through arc lamps, flash lamps or cascaded laser sources. Typical laser sources used in dye laser pumping include frequency-doubled Nd:YAG lasers, CVL, Ar^+, N_2 and excimer lasers. The dye solution is usually pumped transversely through the laser cavity and is contained by a transparent chamber, which is called a flow cell. The broadband laser emissions originate from interactions between the vibrational and electronic states of the dye molecules, which split the electronic energy levels into broad energy bands similar to those of vibrational lasers. In order to tune the laser to a desired frequency, wavelength-selective cavity optics are used (LaserFocusWorld 1995). Dye lasers have high efficiency, good tuning abilities, broadband operation and high spatial coherence.

2.5.6 Other Types of Lasers

Various other types of lasers exist with variations on pump sources and applications. Such lasers include

- FELs,
- gas-dynamic lasers,
- Raman lasers,
- nuclear-pumped lasers, and
- laser-driven plasma accelerators.

A FEL uses high-speed electrons that can move freely in a magnetic field as its lasing medium. These laser types have the largest tunable frequency range of all laser types and span from microwave, THz-radiation, IR, visible and UV to X-ray. The pump source is a relativistic electron beam with emission wavelength (λ_n) from

an undulator[5] with a large number of periods, interference effects in the radiation produced at a large number of essentially co-linear source points in a spectrum with quasi-monochromatic peaks given in Brown et al. (1983) as

$$\lambda_n = \frac{\lambda_u}{2n\gamma^2}\left(1 + \frac{K^2}{2} + \gamma^2\theta^2\right) \quad \text{with } n = 1, 2, 3, \ldots \tag{2.29}$$

where θ is the angle of observation relative to the average electron and direction, n is the harmonic number, λ_u is the spatial period of the magnetic field (the undulator wavelength), γ is the relativistic Lorentz factor and the wiggler strength K is given by

$$K = \frac{eB_0\lambda_u}{\sqrt{8}\pi m_e c} \tag{2.30}$$

where B_0 is the applied magnetic field, m_e is the electron mass, c is the speed of light in a vacuum and e is the electron charge.

Gas-dynamic lasers take a hot and high-pressure mixture of gases, typically CO_2, N_2, H_2O or He, and expand the mixture rapidly through a supersonic outlet. During the expansion the gas is transformed into a laser medium and population inversion is generated. The gas then passes into a laser cavity and the beam is split perpendicular to the flow of the gas through mirrors placed on both ends of the cavity. The gas stream then enters a diffuser where it releases energy and is decelerated to subsonic speeds and exhausted out of the cavity. The non-equilibrium flow through the nozzle and its behavior through the laser cavity determines the distribution of molecules and the conditions where population inversion in the expanding gas occurs. Gas-dynamic lasers are very high-powered and high-efficiency devices with average output power in the hundreds of kWs.

Raman lasers use stimulated Raman scattering to achieve light amplification as opposed to the more traditional electrically induced stimulated transitions. Raman scattering is the inelastic scattering of photons during excitation as opposed to the more general, elastic (Rayleigh) scattering where the photons have the same energy (frequency and wavelength) of the incident photons. Raman lasers are optically pumped, but this optical pumping does not produce population inversion. Pumped photons are absorbed and transitions to lower-frequency laser light. Theoretically, any Raman laser wavelength can be achieved through specifying the pump wavelength, provided both wavelengths are within the transparency region of the material and a sufficiently high non-linearity and/or optical intensity is reached.

If a laser is pumped with energy of fission fragments, it falls under the category of nuclear pumped lasers. The lasing medium is surrounded by a tube lined with uranium-235. To achieve lasing, the medium is subjected to a high neutron flux in a

[5]A periodic structure of dipole magnets forcing electrons to undergo oscillations and resulting in radiated energy.

nuclear reactor core. Nuclear pumped lasers can, for instance, be used to pump X-ray lasers and energize EMP weapons used in EW offensive tactics. Nuclear pumped lasers can scale to very high energy levels, upwards of 100 MW CW beam power, and historically dominates military research. The size and scale of nuclear pumped lasers are extremely large to accommodate the nuclear reactor cores and since these lasers are predominantly CW, the power densities required are very high, but the energy densities emitted are lower compared to electrically charged gas lasers. The most well-known nuclear pumped laser project was Project Excalibur—an X-ray laser used as a DEW for ballistic missile defense. Project Excalibur was officially abandoned in 1992 and research resources were redirected to space-based laser satellite concepts.

Laser-driven plasma accelerators use large electric fields formed within plasma waves to accelerate charged particles to high energies in smaller distances compared to traditional particle accelerators. If a laser pulse propagates through a plasma the non-linear force in an inhomogeneous oscillating electromagnetic field (ponderomotive force) pushes electrons away from the front and back of the pulse and forms a trailing longitudinal density wave. The ponderomotive force in laser-driven plasmas $\mathbf{F}_\mathrm{p}$ in newton is expressed by

$$\mathbf{F}_\mathrm{p} = \frac{e^2}{4m\omega^2}\nabla\left(E^2\right) \tag{2.31}$$

where ω is the angular frequency of oscillation of the electromagnetic field and E is the amplitude of this field. e and m are the electron charge and mass respectively. These forces allow plasma accelerators to achieve acceleration gradients in the order of 100 GeV/m compared to the approximate 100 meV/m of traditional particle accelerators such as the LHC (Esarey et al. 2009). Calculation of the driven electron plasma waves (wakefields) generated by non-evolving drive laser pulses is presented in Esarey et al. (2009).

Optimization of laser technology involves improving on current technologies and laser types to increase the average power output of devices using the same (or lower) power sources. The following section introduces some optimization techniques based on principles that can be applied to most laser types.

2.6 Laser Optimization

Since the early era of laser research and even today, researchers gave pursued various fundamental goals in improving laser technology. These goals are both technology and application specific and aim to improve the throughput and efficiency of laser pumping through a variety of applications. No single laser can satisfy all the requirements for the vast applications of lasers and research into improving single laser technologies for their associated applications is necessary. A list of general goals of laser advances are improving on

- the type of applications requiring different spectra of luminous light and finding efficient and cost-effective ways to implement it,
- technology advances aimed at increasing the maximum average output power of laser types,
- technology advances aimed at increasing the energy of the peak pulse,
- increasing the output power of the peak pulse,
- improving on the enabling technologies and supporting circuitry to allow higher frequency laser pulse throughput,
- techniques for achieving higher power efficiency, and
- ultimately lowering the cost and decreasing the physical size of lasers.

The classification of lasers differs on the intended end-use of the laser; however, the most general classification that reveals most information is considered to be the state of the lasing medium (gas, solid or liquid). Another consideration when classifying a laser, albeit a somewhat reversed methodology, is classification by its wavelength of operation. This is, however, a common way to determine which laser is right for a certain application when the intended application defines the wavelength required and the type of lasing medium is chosen based on this requirement. Bhatia and Kumar (2002) further classified laser types in terms of their susceptibility to EMI and lists categories that influence interference in operation:

- The physical construction of the laser is decisive; Bhatia and Kumar (2002) stated that more voluminous and longer dimensioned laser tends to be better suited for radiated EMI emissions.
- High-powered lasers contribute to larger conducted noise levels and the operating power as a function of input power should be limited through more efficient lasers.
- Considering the operating mode, CW lasers are generally less noisy compared to their pulsed mode counterparts because of the lower frequency activity in its electrical drivers. Pulsed lasers, especially very high frequency/short pulses, contribute more to noise at the output;
- The optical pumping method influences the generated noise and interference in the laser output and it is generally found that gas lasers, because of their complex electrical requirements and high frequencies, generate higher levels of noise compared to for example flash lamp pumping.
- Any additional accessories used for the laser pumping and supporting circuitry adds to the generated noise levels in the output signal.

Chen et al. (1996) highlight the fact that in optically coupled lasers, the pump source and the laser resonator do not interfere with each other (optical versus electrical characteristics), which lowers the total output noise of the system. Also mentioned is the fact that a fiber-coupled system has significantly lower brightness, since the brightness of the output beam is always lower or at best equal to the brightness of the input beam, measured in $W/cm^2.sr$ (where steradian (sr) is the unit of the solid angle). Chen et al. (1996) found that the optimum focus position of the

pumping light in optically coupled systems depends on the pump-beam quality, pump spot size and the laser mode size.

In optically pumped lasers the slope efficiency σ_s (or differential efficiency) is typically used to determine the efficiency of the output power (P_{out}) versus the pump power (P_{in}) of the laser. If third-order effects such as quasi-three-level characteristics of the gain medium or other thermal effects do not dominate laser operation, the slope efficiency plots are generally linear. If the slope efficiency curve displays significant non-linear behavior due to, for example, thermal lensing or overheating of the gain medium, the slope is often determined in pre-defined and normal operating condition sections. The gradient of a non-linear efficiency curve is primarily determined by

- the power of the beam passing through the output mirror compared to the total losses in the cavity, and
- the ratio (between 0.0 and 1.0) of the pump wavelength to the laser wavelength.

Slope efficiency graphs also have a distinct point on the pumping power axis where the output power becomes a non-zero value and this point is referred to as the oscillation threshold (P_{th}). The optimization of the laser output power involves trade-offs between high slope efficiency and low threshold pump power. A typical slope efficiency graph is given in Fig. 2.12.

The efficiency slope as shown in Fig. 2.12 can be determined through

$$\sigma_s = \frac{P_{in} - P_{th}}{P_{out}} \frac{(hv)_{laser}}{(hv)_{pump}} \tag{2.31}$$

where $(hv)_{laser}$ and $(hv)_{pump}$ are the wavelengths of the laser and the pump respectively. The highest theoretical slope efficiency could exist if the pump wavelength and the laser wavelength are exactly equal and the slope in Fig. 2.12

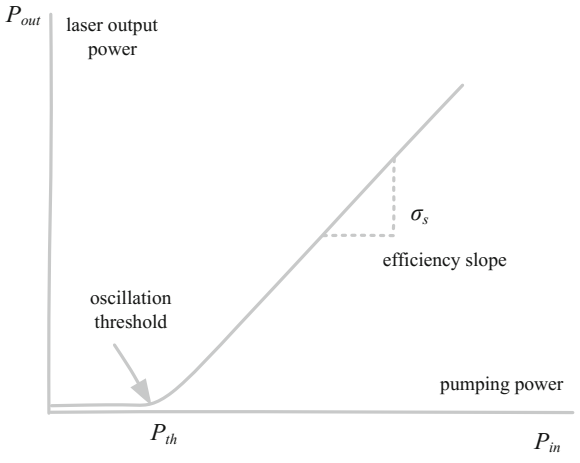

Fig. 2.12 A typical linear slope efficiency curve of pumping power versus output power in optically-pumped lasers

equals 45°. Practically, slope efficiencies are in the range of 5 % or less and can reach up to 30 % for diode pumped lasers. Laser diode performance parameters and experimental procedures to determine and interpret certain parameters are given in Mobarhan (1999). The laser diode parameters include:

Output light versus input current and threshold current: This parameter can be considered one of the most important characteristics of a laser diode, describing the magnitude of the light emitted by the laser as a current injected into the device. The commonly used output light power (P_{out} in watts) versus input current (I_{in} in amperes) (known as the LI curve, which is similar to the efficiency slope) curve is generated by measuring the stimulated radiation to the input current. The LI curve also has a threshold current $I_{th,}$ where the device starts radiating. The slope of the curve is determined by the ratio of $\Delta P_{out}/\Delta I_{in}$ at its nominal operating points, determining its effective slope efficiency in this way. Ideally a diode laser should only require small variations in input current for large variations in output light power, therefore have a large slope efficiency. The LI curve is also typically a linear curve except if third-order effects are dominant during operation at the limits of the device, particularly above the threshold current position and below its maximum input current rating.

Threshold current density: The threshold current of the laser diode, I_{th}, is a factor of the quality of the semiconductor material and the geometric design of the optical waveguide. It furthermore depends on the size and the absolute area of the diode laser—important to consider when comparing lasers, since a higher threshold current could be purely due to a larger device. To avoid confusion in directly comparing threshold current between devices that may occupy a larger or smaller area, the threshold current density J_{th} is used instead. J_{th} is a better indication of the quality of the semiconductor material from which the device is manufactured. The transparency threshold current density (J_O) is used to compare threshold current density between different batches of semiconductor processes. J_O is found by plotting threshold current density versus the inverse of optical cavity length and finding the intersection with the vertical axis of the linear fit line of the data points. J_O can therefore be regarded as the threshold current density of a theoretically infinitely long laser cavity with no losses at its mirror facets used to compare semiconductor process characteristics during diode laser manufacturing.

External differential quantum efficiency: This figure of merit (FOM) parameter of a device indicates the efficiency of the device to convert injected electron-hole pairs to photons emitted from the device (Mobarhan 1999). The external differential quantum efficiency (η_d) can be determined by the slope efficiency with

$$\eta_d = \frac{P_{out}}{I_{in}} \frac{q\lambda}{hc} \tag{2.32}$$

where q is the elementary electron charge (1.6×10^{-19} C). In (2.32) the term P_{out}/I_{in} has units W/A and $q\lambda/hc$ has units A/W—therefore the external differential quantum efficiency is unit-less—a percentage of injected electron-hole pairs converted to actual emitted radiative photons. Mobarhan (1999) also highlights the

importance of specifying the type of laser in terms of wavelengths emitted and number of reflective mirrors, since these parameters influence the absolute slope efficiency that can be achieved in a system.

Cavity length dependence on J_{th} and η_d: In order to determine a viable average of the threshold current density and the external differential quantum efficiency for various cavity lengths and to define the material quality and semiconductor process for a batch of laser diodes accurately, a variety of cavity lengths should be measured and compared. Having broad area lasers with clearly defined geometries simplifies these measurements to determine the average values.

Internal quantum efficiency: This parameter, η_i, specifies the efficiency of a diode laser to convert electron-hole pairs into photons within the diode structure itself (not accounting for actual radiated photons) independently of the geometrical properties of the device. The inverse of the internal quantum efficiency is a measure of the injected current converted into other forms of energy, such as thermal energy (heat) and not applied to light photons. To eliminate the influence of cavity length on the efficiency to convert electron-hole pairs to photons, η_i is typically determined by plotting the external differential quantum efficiency versus the cavity length and finding the inverse of the intercept point of the linear fit line from the set of data points with the vertical axis. Graphically, this procedure is presented in Fig. 2.13.

The external differential quantum efficiency is always less than, based on a value of between 0 and 1, the internal quantum efficiency, since not all photons generated in the device ultimately exit the device again as radiated photons and can become trapped or lost inside the device. The ratio of η_d/η_i specifies the number of photons emitted from the laser to the number of photons generated in the laser (Mobarhan 1999).

Characteristic temperature: High-powered lasers inevitably cause the operating temperature of the device to rise. The temperature sensitivity T_0 of the device specifies the amount of change in external differential quantum efficiency and threshold current density with increasing temperature and translates to the thermal stability of the device. T_0 can be determined by

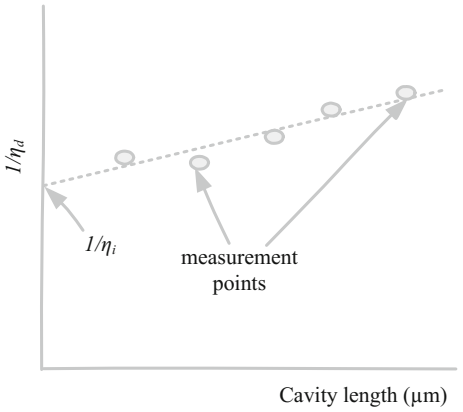

Fig. 2.13 Determining the internal quantum efficiency of a diode laser from the external differential quantum efficiency and the cavity length

$$T_0 = \frac{\Delta T}{\Delta \ln(J_{th})} \tag{2.33}$$

where ΔT is the difference in temperature between two measurements of measured/calculated threshold current density J_{th}.

Spectrum and peak wavelength: The number of spectral outputs that a laser is capable of emitting is a function of the optical cavity structure and the operating current (Mobarhan 1999). As a result, multimode lasers exhibit multiple spectral outputs around their center wavelength. Optical cavity lengths are designed with respect to the output wavelength and are typically chosen at lengths of $\lambda/2$ multiplied by the oscillations, m. The center wavelength of a laser diode is also proportional to the temperature where the output wavelength increases with increasing temperature. This becomes a useful characteristic of laser diodes when tunable lasers are required. The output wavelength can in addition be tuned by changing the input current, generally displaying discrete changes in wavelength. This phenomenon is known as mode hopping and is evident in single-frequency laser diodes.

The following paragraph concludes the discussion on particle accelerators and laser physics, types and optimizations.

2.7 Conclusion

This chapter focuses on particle acceleration technology, its history and its contribution to other technologies such as lasers. Lasers are found in various applications, commercial and military, and this chapter introduces the basic principles of lasers, the types of lasers and laser optimization. In the following chapter, the supporting circuitry to drive lasers is discussed, with the emphasis on the role of SiGe in these devices. The following chapter further investigates the uses of fast-switching, low-noise, compact and efficient SiGe laser drivers in military applications, such as laser rangefinders, laser DEWs, IR countermeasures (IRCM) and laser detonators.

References

Barbalat, O. (1994). Applications of particle accelerators. *CERN-AC-93-04-BLIT-REV*. CERN, 1994.

Bäuerle, D. W. (2013). Laser processing and chemistry. *Springer Science & Business Media*, 29 June 2013.

Benson, R. C., & Mirarchi, M. R. (1964). The spinning reflector technique for ruby laser pulse control. *IEEE Transactions on Military Electronics, 8*(1), 13–21.

Bhatia, M. S., & Kumar, G. (2002). On the EMI potential of various laser types. In *Proceedings of the Electromagnetic Interference and Compatibility* (pp. 3–5).

Bhawalkar, D. D., Gambling, W. A., & Smith, R. C. (1964). Investigation of relaxation oscillations in the output from a ruby laser. *Radio and Electronic Engineer*, *27*(4), 285–291.

Brown, G., Halback, K., Harris, J., & Winick, H. (1983). Wiggler and undulator magnets—A review. *Nuclear Instruments and Methods*, *208*(65–77), 1983.

CERN. (2009). CERN LHC: The guide. Retrieved Jan 21, 2016 from http://cds.cern.ch

Chen, Y. F., Liao, T. S., Kao, C. F., Huang, T. M., Lin, K. H., & Wang, S. C. (1996). Optimization of fiber-coupled laser-diode end-pumped lasers: Influence of pump-beam quality. *IEEE Journal of Quantum Electronics*, *32*(11), 2010–2016.

Coldren, L. A., Fish, G. A., Akulova, Y., Barton, J. S., Johansson, L., & Coldren, C. W. (2004). Tunable semiconductor lasers: A tutorial. *Journal of Lightwave Technology*, *22*(1), 193–202.

Einstein, A. (1905). Does the inertia of a body depend upon its energy-content? *Translated from Annalen der Physik, 18*(639), 1905.

Endo, M., & Walter, R. F. (2006). *Gas lasers*. CRC Press, 26 Dec 2006.

Esarey, E., Schroeder, C. B., & Leemans, W. P. (2009). Physics of laser-driven plasma-based electron accelerators. *Reviews of Modern Physics, 81*(3), 1229–1280.

Evtuhov, V., & Neeland, J. K. (1965). Study of the output spectra of ruby laser. *IEEE Journal of Quantum Electronics*, *1*(1), 7–12.

Gilmore, R. (2004). *Elementary quantum mechanics in one dimension*. USA: JHU Press.

Gulley, J. R. (2011). Modeling free-carrier absorption and avalanching by ultrashort laser pulses. In *Proceedings of SPIE*. 8190 819022-1-112011.

Ivey, H. F. (1966). Electroluminescence and semiconductor lasers. *IEEE Journal of Quantum Electronics*, *2*(11), 713–726.

Javan, A., Bennet, W. R., & Herriott, D. R. (1961). Population inversion and continuous optical maser oscillation in a gas discharge containing a He-Ne mixture. *Physical Review Letters, 6* (106–110), 1961.

Kelsall, R. W., & Soref, R. A. (2003). Silicon-Germanium quantum-cascade lasers. *International Journal of High Speed Electronics and Systems*, *13*(2), 197–223.

Knochenhauer, C., Hauptmann, S., Scheytt, C., & Ellinger, F. (2009). A compact, low-power 40 Gbit/s differential laser driver in SiGe BiCMOS technology. In *2009 European Microwave Integrated Circuits Conference* (pp 324–326).

Laser Enterprise. (2016). Retrieved Feb 4, 2016 from http://www.laserenterprise.com/

LaserFocusWorld. (1995). Retrieved Feb 4, 2016 from http://www.laserfocusworld.com

Maiman, T. H. (1960). Stimulated optical radiation in ruby. *Nature, 187*, 493–494.

Marshall, W. K., & Burk, B. D. (1986). Received optical power calculations for optical communications link performance analysis. *TDA Progress Report*. 42–87, July–Sept 1986.

Mobarhan, K. S. (1999). Application note: Fiber optics and photonics. Test and characterization of laser diodes: Determination of principal parameters> *Newport Application Note*.

Moto, A., Ikagawa, T., Sato, S., Yamasaki, Y., Onishi, Y., & Tanaka, K. (2013). A low power quad 25.78-Gbit/s 2.5 V laser driver using shunt-driving in 0.18 μm SiGe-BiCMOS. In *2013 IEEE Compound Semiconductor Integrated Circuit Symposium (CSICS)* (pp. 1–4).

Nathan, M. I., Dumke, W. P., Burns, G., Dill, F. H., & Lasher, G. (1962). Stimulated emission of radiation from GaAs p-n junctions. *Applied Physics Letters*, *1*, 62–64, Nov 1962.

Oxborrow, M., Breeze, J. D., & Alford, N. M. (2012). Microwave laser fulfills 60 years of promise. *Nature*, *488*, 353–356.

Patel, C. (1984). Lasers—their development and applications at AT&T bell laboratories. *IEEE Journal of Quantum Electronics*, *20*(6), 561–576.

Photonics Handbook. (2015) Retrieved Feb 3, 2016 from http://www.photonics.com/

Porto, S. P. S. (1963). A simple method for calibration of ruby laser output. In *Proceedings of the IEEE*, *51*(4), 606–607.

Quist, T. M., Rediker, R. H., Keyes, R. J., Krag, W. E., Lax, B., McWhorter, A. L., et al. (1962). Semiconductor maser of GaAs. *Applied Physics Letters*, *1*, 91–92.

Seo, D-K., & Hoffmann, R. (1999). Direct and indirect band gap types in one-dimensional conjugated or stacked organic materials. *Theoretical Chemistry Accounts*, *102*, 23–32.

Silfvast, W. T. (2004). Laser fundamentals. In *School of Optics: University of Central Florida* (2nd ed.). Cambridge: Cambridge University Press.

Tauc, J. (1968). Optical properties and electronic structure of amorphous Ge and Si. *Materials Research Bulletin*, *3*(1), 37–46.

Townes, C. H. (1965). 1964 Nobel lecture: Production of coherent radiation by atoms and molecules. *IEEE Spectrum*, *2*(8), 30–43.

Tsujino, S., Scheinert, M., Sigg, M., Grutzmacher, D., & Faist, J. (2006). Strategies to improve optical gain and waveguide loss in SiGe quantum cascade devices. In 2nd *IEEE International Conference on Group IV Photonics* (pp. 4–6).

Woodyard, J. R. (1948). High-particle accelerators. *Electrical Engineering, 67*(8), 759–767.

Yariv, A., & Gordon, J. P. (1963). The Laser. In *Proceedings of the IEEE*, *51*(1), 4–29.

http://www.springer.com/978-3-319-47402-1

SiGe-based Re-engineering of Electronic Warfare Subsystems

Lambrechts, W.; Sinha, S.

2017, XX, 329 p. 118 illus., Hardcover
ISBN: 978-3-319-47402-1